FOOT dE/dx detector: simulation report

Matteo Bertazzoni, Maria Giuseppina Bisogni, Esther Ciarrocchi e Matteo Morrocchi

February 16, 2017

1 Introduction

The goals of the dE/dx detector group are to determine the energy and time resolution of the dE/dx detector and to optimize the geometry by means of measurements and Geant4 simulations (Agostinelli et al., 2003). The simulation models the geometry of a prototype of the dE/dx detector (i.e., a single scintillating bar coupled at the two ends to two SiPMs via two light guides) and the optical transport of the scintillation photons inside the bar. In the final version of the simulation, the input to the code will be the amount of energy released by the ion in the scintillator bar (provided by the Fluka simulation group). The simulation outputs are the fraction of photons detected by the SiPMs at the two ends of the bar and their arrival time. The analog signal of the SiPM is then modeled with Matlab custom code to obtain the energy and time resolution of the full detection system. The simulations will be tuned and validated with acquisitions using both a lab sealed β-source and a real therapeutic beam.

2 Materials and Methods

2.1 dE/dx detector geometry

In the current version of the simulation, the detector is composed by (Fig. 1):

- a plastic scintillator bar (EJ212, produced by Eljen Technology), with dimensions 20 mm × 3 mm × 40 mm;

- two trapezoidal Plexiglass optical guides (larger base 20 mm × 3 mm, smaller base 3 mm × 3 mm and 14.94 mm height, to give a 60°focusing angle) wrapped with 200 μm of Aluminum;
- two SiPM photodetectors (NUV, produced by AdvanSiD) simulated with a 3mm× 3 mm × 1 mm silicon box;
- 100 μm layers of optical grease (Saint-Gobain BC-630) to couple the optical guides to both the scintillator bar and the SiPM.

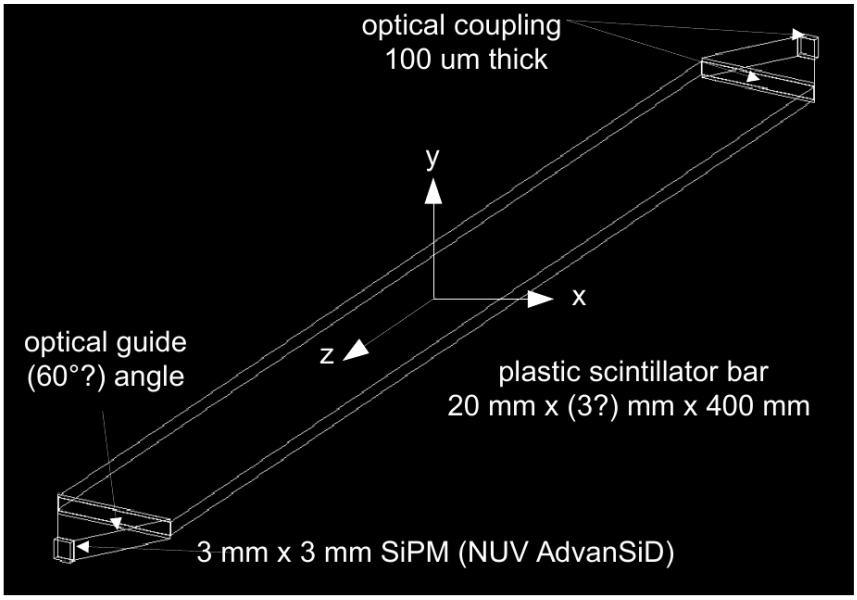

Figure 1: Geometry of the FOOT dE/dx detector.

All volumes are immersed in vacuum. This preliminary simulation is used for a rough estimate of the detector performance. The tuning of the simulation parameters will be performed with a detector prototype featuring a 200 mm long EJ212 bar, which is already available in our lab. In the final version of the detector, the plastic scintillator will be replaced by a 400 mm long Saint-Gobain BC-408 bar (or any of the equivalent scintillators commercially available), and the simulation validation will be performed with this final scintillator.

Scintillator specifications The specifications of the scintillator currently implemented in the simulation are reported in Table 1 (the rise time still needs to be modeled).

The emission spectrum of the scintillator shown in Figure 2 was sampled as a function

Table 1: Properties of EJ212 scintillator bar currently simulated.

Scintillation efficiency	10^4 photons/MeV
Visible light attenuation length	250 cm
Rise time	0.9 ns
Decay Time	2.4 ns
Density	1.023 g/cm^3
Polymer base	Polyvinyltoluene
Refractive index	1.58

of wavelength and included in the code. Scintillation photons are simulated in the scin-

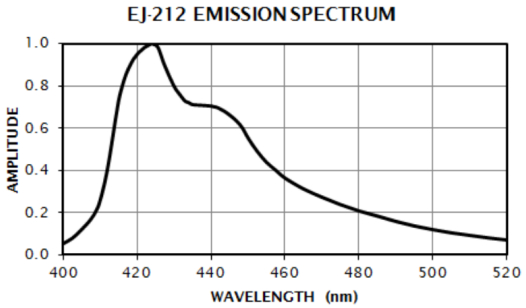

Figure 2: Emission spectrum of the EJ212 scintillator bar currently simulated.

tillator wavelength emission range ($\lambda = 400 - 520$ nm), and materials optical properties were included for this same range. The scintillator emission has not yet been corrected for the relative light yield of 100 MeV proton with respect to electrons.

SiPMs specifications The used SiPMs are NUV by AdvanSid (Fig. 3-left), with the features described in Table 2. The NUV photon detection efficiency (PDE) shown in Fig. 3-right was sampled as a function of wavelength and included in the simulation.

Optical interfaces Two types of optical interfaces are available in Geant4:

- *dielectric-metal*: the photon can be absorbed by the metal or reflected back into the dielectric; if it is absorbed, it can be detected according to the photoelectron efficiency of the metal (when this parameter is specified).

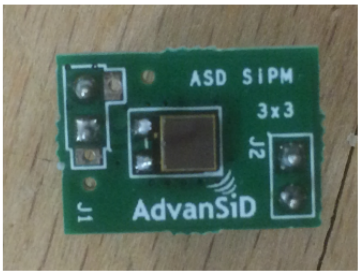

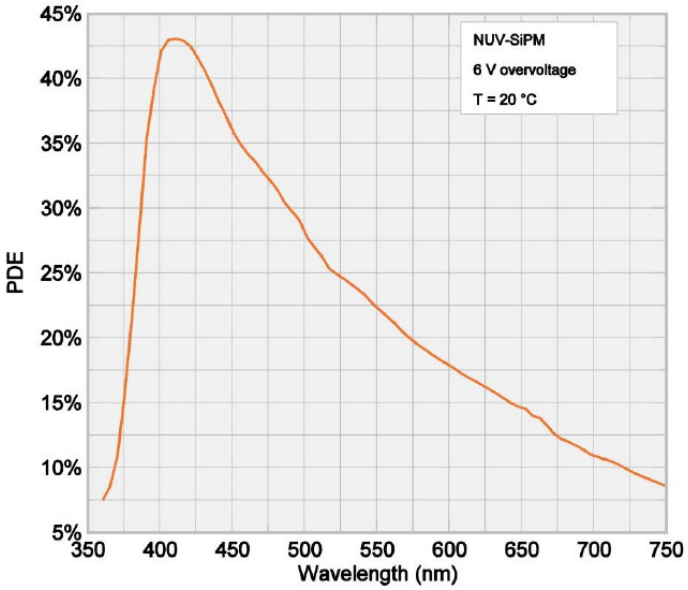

Figure 3: Left: Picture of an AdvanSiD NUV SiPM. Right: Typical photon detection efficiency of an AdvanSiD NUV SiPM.

Table 2: Properties of the SiPM AdvanSiD NUV SiPM. V_{over} denotes the overvoltage (excess bias over breakdown voltage).

Effective active area	3 mm × 3 mm
Number of cells	5520
Breakdown voltage	∼26 V
Gain (at 5 V_{over})	$3.25 \cdot 10^6$
Dark count rate	∼900 kHz
Crosstalk probability	22%
Afterpulse probability	<4 %

- *dielectric-dielectric*: based on the refractive indexes of the two materials and on the photon angle of incidence, the photon may be subject to total internal reflection, Fresnel reflection or refraction.

Any material with no defined refractive index is treated as a metal by Geant4, while for any dieletric, Fresnel's laws are automatically applied based on the media refractive indexes. In addition, the user can define a physical object, called *optical surface*, to specify additional optional information on the optical interface. There are two models to describe optical interfaces, and we use the most recent and general one, called *unified* as it models different types of reflection by means of cross-correlated probability coefficients (Levin and Moisan, 1996). In addition, for a defined optical surface, the surface finish can be chosen among several options. For example it can be smooth (*polished*) or rough (*ground*); other finish options are available but have not been considered yet in the simulation.

The values of refractive index assigned to the different simulated materials are summarized in Table 3. In the current version of the simulation, the interface between

Table 3: List of refractive indexes of the simulated materials, assumed constant in the simulated wavelength range $\lambda = 400 - 520$ nm.

Material	**n**	**Reference**
Vacuum	1.000	Wikipedia for Air
Aluminum	1.440	Vraywiki, openfisica
Plexiglass	1.491	Wikipedia
Scintillator	1.580	Producer website
Optical grease	1.465	Producer website

scintillator and vacuum is modeled as a *dielectric-metal, polished* interface, and reflectivity is set to $R = 98\%$. In this way, all photons that are not reflected are automatically absorbed (and killed). All of the remaining interfaces but the one between optical grease and SiPM (e.g, between scintillator and optical grease, between optical grease and light guide, between light guide and optical grease, between optical grease and vacuum and between light guide and vacuum) follow Fresnel laws of reflection and refraction based on the materials refractive indexes. The interface between optical grease and SiPM

is modeled as a *dielectric-metal* one, and a detection efficiency is assigned to record detected photons.

2.2 Event simulation

In the current version of the simulation, the primary beam is a proton beam of given energy (e.g., 100 MeV) that is launched in the y-direction (see Fig. 1). The energy released by the primary particle in the scintillator bar is saved at the end of the interaction to normalize the simulation output for this value. A total of $N = 10^3$ primary particles are simulated. The beam position is varied along the z-direction to determine the effect on the energy and time resolution of different interaction positions.

2.3 Variable input parameters

Since the simulation will be used to optimize the geometry of the dE/dx detector and to study the effects on the time and energy resolution, the geometry modeling is parametrized to allow to easily vary several input parameters, such as the angle of the optical light guide, the reflection coefficient of the wrapping material and the scintillator properties (e.g., time constants and light yield).

Based on their Fluka simulation of the energy release in the bar, the Fluka simulation group has noted that part of the fragmentation events take place inside the scintillator, thus degrading the energy resolution, especially for low charge values. This phenomenon could be limited by reducing the scintillator bar thickness, although degrading the time resolution. One possible solution could be to use a set of two bars, a first thin one for the energy information followed by a thicker one for the time information. For this reason, also the thickness of the scintillator bar (i.e., its y-dimension) is varied between 1 and 3 mm to study its impact on the number of detected photons and on their time of arrival in the SiPM.

Up to date, the following values of the variable parameters have been simulated: scintillator thickness $y = 1, 2, 3$ mm and beam position $z = 0, 50, 100$ mm.

2.4 Optimization of the simulation

One major issue that emerged from the first runs is the computational cost of the optical photons tracking: the simulation of the 3 mm thick bar requires more than 6 hours for 10^3 primary particles. One possible solution to reduce the time consumption is to include the Monte Carlo simulation in a semi-analytical model of the detector, as done by (Derenzo, Choong, and Moses, 2014). The idea is to factorize the detector response in an analytical component, which can be easily modeled also in MatLab, for example, and in a stochastic component, necessarily requiring a Monte Carlo description.

The first analytical component is the emission of the scintillation photons, described by the difference of two exponential functions of time as follows:

$$f(t) = \frac{N_{det}\left(\mathrm{e}^{-t/\tau_d} - \mathrm{e}^{-t/\tau_r}\right)}{\tau_d - \tau_r} \tag{1}$$

where N_{det} is the number of detected photons (whose determination will be explained later), and $\tau_{r,d}$ are the scintillator rise and decay time, respectively.

The second analytical component is the contribution of the light guide, which is also and exponential function of time:

$$g(t) = \frac{\mathrm{e}^{-t/d}}{d} \tag{2}$$

where d is a delay which depends on the reflectivity and dimensions of the bar.

The number of detected photons in (1) can also be factorized as follows:

$$N_{det} = F(E, LY) \cdot DE \cdot OT \tag{3}$$

where $F(E, LY)$ is a function of the energy released in the bar E (provided by the Fluka simulation) and of the light yield LY of the scintillator (which is a known value and should also account for the scintillator saturation), the efficiency of the optical transport OT (which is the output of the Geant4 simulation) and the detection efficiency DE which is the product of the photon detection efficiency of the photodetector and of the

emission spectrum of the scintillator (which are also provided by the producers)[1]. The optical transport efficiency OT depends on the absorption probability in the bulk of the material $s_{abs}(z)$, on the probability of absorption at optical interfaces $P_{int}(z)$ (due to the incomplete reflectivity of the wrapping material) and on the light guide efficiency LG:

$$OT = s_{abs}(z) \cdot P_{int}(z) \cdot LG \tag{4}$$

(assuming that losses due to non-perfect optical coupling are negligible, at least in first approximation). The absorption in the bulk of the bar and at the interfaces can be modeled again by analytical exponential functions:

$$s_{abs}(z) = \mathrm{e}^{-|x_0 - z|/l_{abs}}, \quad P_{int}(z) = \mathrm{e}^{-|x_0 - z|/l_{int}} \tag{5}$$

where $x_0 - z$ is the distance between the photosensor and the interaction position of the primary particle, the scintillator light absorption length l_{abs} is provided by the producer and l_{int} should be determined by the simulation, using the real reflection coefficient of the wrapping. The remaining factors in (4) are the ones that should be provided by the Monte Carlo simulation.

2.5 Generation of the SiPM analog signal

The arrival time of the optical photons in the two SiPMs is further elaborated with MatLab custom code to model the SiPM analog signal. First the mean signal of the SiPM is modeled using dark measurements (Fig. 4-left). The number of photons produced by dark events corresponding to this mean signal are not known, therefore the mean signal is multiplied for a rescaling factor to obtain the single-photon signal. The rescaling factor accounts for the SiPM gain at the applied overvoltage value, for the 50 Ω input resistance of the oscilloscope and for the area of the mean measured dark event area. The normalized mean signal is then summed for each time-stamp provided by the simulation to obtain the total simulated signal. Then, dark noise is added to the total signal,

[1] assuming that crosstalk and afterpulse effects are included in a later moment with other detector-related noise components, as done here.

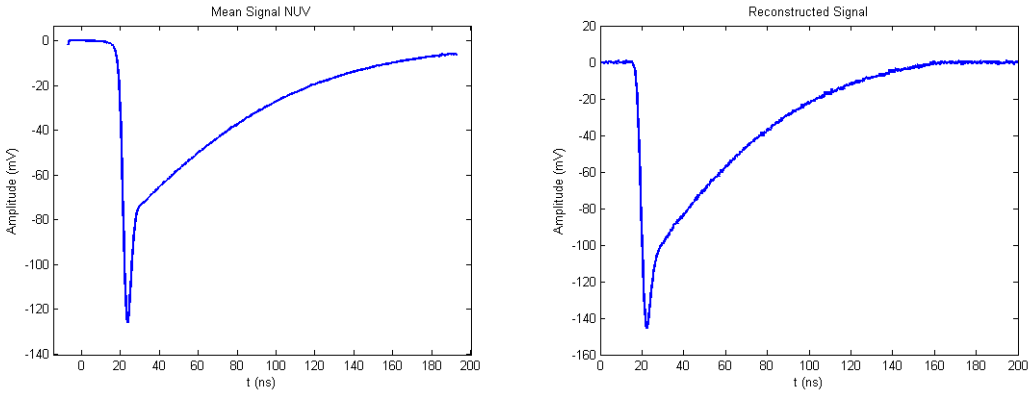

Figure 4: Left: Mean signal of a NUV SiPM. Right: Simulated total NUV SiPM signal.

as well as the contribution of crosstalk and electronic noise. An example of the final reconstructed signal is shown in Fig. 4-right.

3 Results and discussion

3.1 Detection efficiency

Figure 5 shows the distribution of the fraction of scintillation photons detected by the two SiPMs (i.e., the sum of the photons detected in the two photosensors divided by the total number of generated photons), for $N = 10^3$ primary particles and for bars of different thickness: 1 mm (left), 2 mm (center), 3 mm (right).

The fraction of collected photons at one side of the bar is shown in Fig. 6 as a function of the distance of the beam interaction position from one end of the bar, for three bar thickness values. The three lines show an exponential fit of the curves, suggesting a possible exponential attenuation. However, plastic scintillator producers (e.g., Saint-Gobain) report deviations at the edges of the bar, and this region will be investigated with other runs.

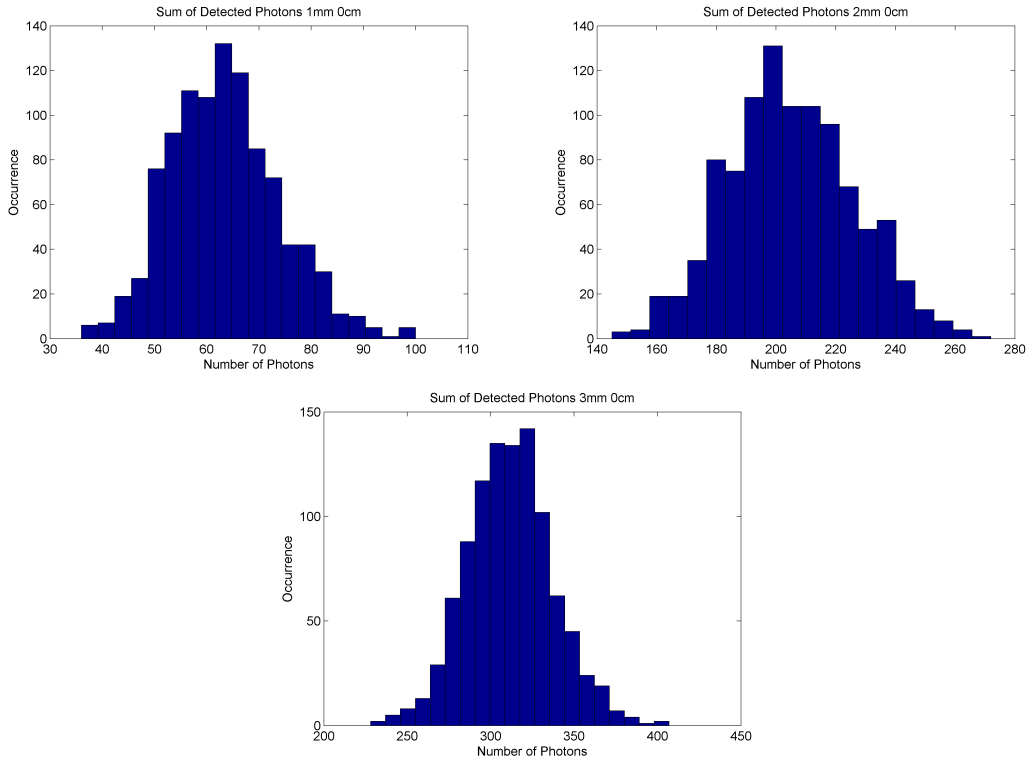

Figure 5: Detector sensitivity: fraction of detected scintillation photons for bars of different thickness: 1 mm (left), 2 mm (center), 3 mm (right).

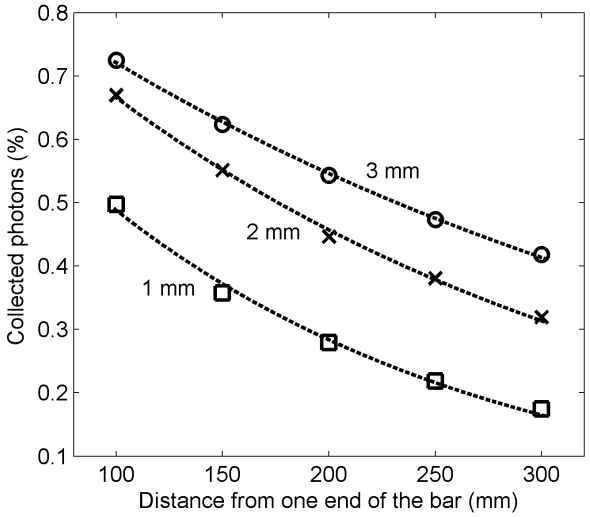

Figure 6: Percentage of detected scintillation photons as a function of the beam interaction position with respect to one end of the bar, for bars of different thickness.

3.2 Time of flight information

Figure 7 shows the statistical distribution of the time of arrival of the $n-th$ photon on the two SiPMs, for $n = 1-5$ (different colors) and for the beam position $z = 0$ mm, corresponding to the center of the scintillator, and for three bar thickness values (three plots). Simulations for more positions are being run and results will be available soon.

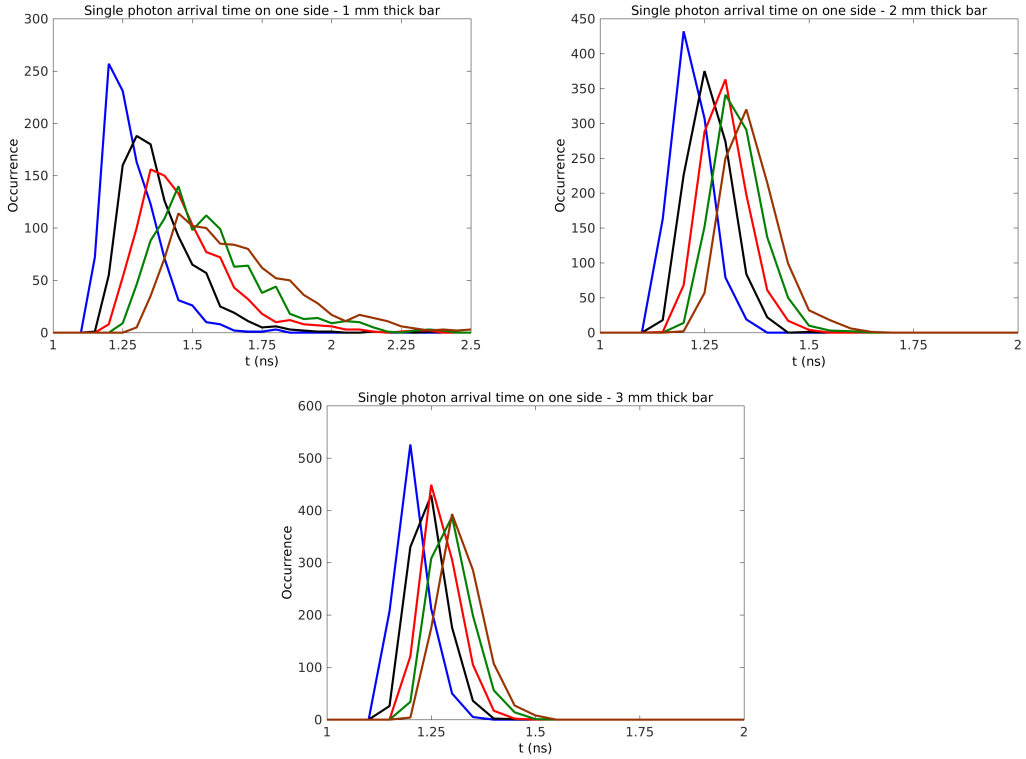

Figure 7: Statistical distribution of the time of arrival of the $n-th$ photon on the two SiPMs, when the beam is launched at the center of the scintillator ($z = 0$ mm, left), for $n = 1-5$ (different colors) and for three bar thickness values.

The top row of Fig. 8 shows the mean time of arrival of the $n-th$ photon on the two SiPMs, for the 1 mm thick bar and for the beam positions $z = 0$ mm, corresponding to the center of the scintillator. The bottom row shows the standard deviation of the arrival times. Simulations for more positions are being run and results will be available soon. Figures **??** show the same results for the 2 and 3 mm thick bars.

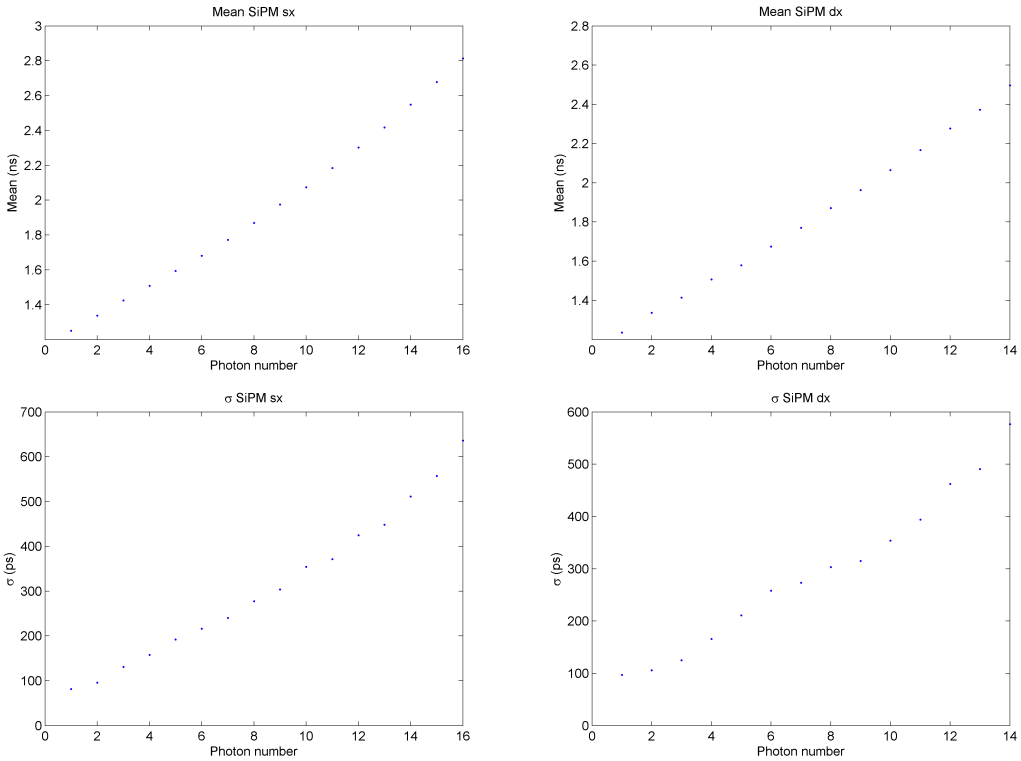

Figure 8: Top: Mean time of arrival of the $n-th$ photon on the two SiPMs, when the beam is launched at the center of the scintillator ($z = 0$ mm, left) and the bar is $y = 1$ mm thick. Bottom: Standard deviation of the arrival time.

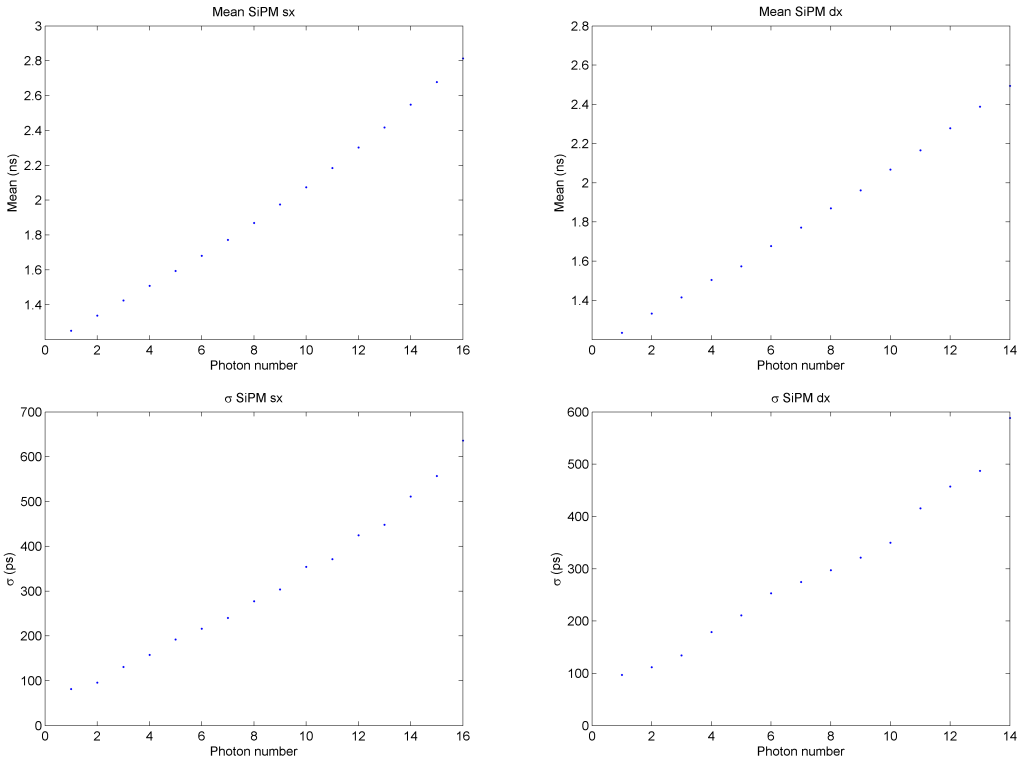

Figure 9: Top: Mean time of arrival of the $n-th$ photon on the two SiPMs, when the beam is launched at the center of the scintillator ($z = 0$ mm, left) and the bar is $y = 2$ mm thick. Bottom: Standard deviation of the arrival time.

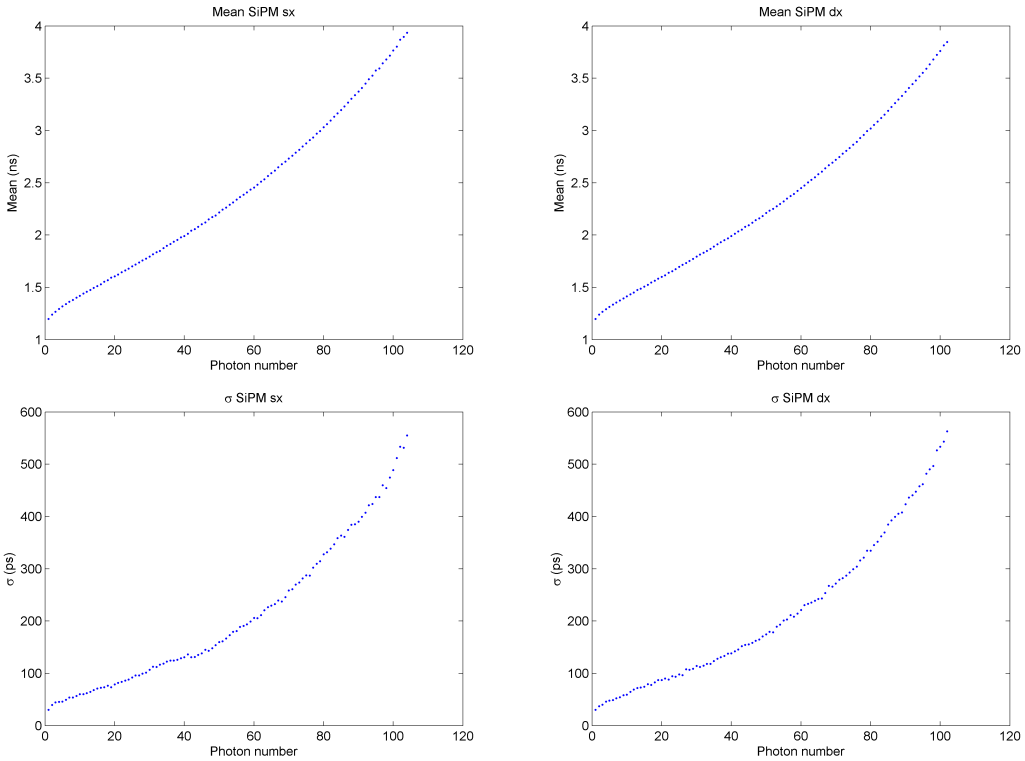

Figure 10: Top: Mean time of arrival of the $n-th$ photon on the two SiPMs, when the beam is launched at the center of the scintillator ($z = 0$ mm, left) and the bar is $y = 3$ mm thick. Bottom: Standard deviation of the arrival time.

3.3 Energy information

Table 4 summarizes some of the factor determining the energy resolution: $\mu(N_{gen})$ is the mean of the distribution of the number of generated scintillation photons, $\sigma(N_{gen})$ is its standard deviation, $\mu(N_{det})$ is the mean number of detected photons (the total at the two photodetectors), $\sigma(N_{det})$ is its standard deviation, and $P_{det} = \mu(N_{det})/\mu(N_{gen})$ is the detection probability.

Table 4: Figures of merit in the energy resolution.

z (mm)	N_{gen}		N_{gen}		P_{det} (%)
	μ	σ	μ	σ	
1	11464	1200	64	11	0.56
2	22853	1700	205	21	0.90
3	28707	1800	312	26	1.08

The energy resolution values are reported in Table 5: $\text{Res}_{det} = \frac{1}{N_{det}}\sqrt{N_{gen}P_{det}(1-P_{det})} = \frac{1}{N_{gen}}\sqrt{(1-P_{det})/P_{det}}$ is the contribution of the detector, including the optical transport in the bar, the absorption of the scintillator and of its wrapping, the effect of the light guide and the photon detection efficiency (PDE) of the detector (see 2.4)[2]; $\text{Res}_{det+stat}$ is the sum of Res_{det} and the statistical fluctuations in the generation of the scintillation photons; $\text{Res}_{sim} = \sigma(N_{det})/\mu(N_{det})$ is the resolution obtained by the simulation, expected to equal $\text{Res}_{det+stat}$.

Table 5: Energy resolution: contribution of the detector (Res_{det}), calculated sum of detector contribution and statistical fluctuations ($\text{Res}_{det+stat}$), corresponding simulated resolution (Res_{sim}).

z (mm)	Res_{det} (%)	$\text{Res}_{det+stat}$ (%)	Res_{sim} (%)
1	12.6	16.4	17.2
2	7.0	10.2	10.2
3	5.6	8.4	8.3

[2]The detector noise (i.e., crosstalk and afterpulse) is not included yet in the results shown in Table 5.

4 Conclusions and future work

Conclusions The simulation platform for the modeling of the optical transport in the dE/dx detector is almost ready, and first preliminary results were presented. The tuning and validation will be performed as soon as the experimental setup will be available.

Future work The simulation parameters will be first tuned used the detector prototype available in our lab (with the short EJ212 bar). The impact on the energy and time resolution of several factors will be evaluated: beam interaction position and type of particle, bar reflection coefficient, rise-time and thickness, number of scintillation photons produced in the event. The simulation will then be validated with the final detector (beam test scheduled for next June).

References

Agostinelli, Sea et al. (2003). "GEANT4-a simulation toolkit." In: *Nuclear instruments and methods in physics research section A: Accelerators, Spectrometers, Detectors and Associated Equipment* 506.3, pp. 250–303.

Derenzo, Stephen E, Woon-Seng Choong, and William W Moses (2014). "Fundamental limits of scintillation detector timing precision." In: *Physics in medicine and biology* 59.13, p. 3261.

Levin, A and Christian Moisan (1996). "A more physical approach to model the surface treatment of scintillation counters and its implementation into DETECT." In: *Nuclear Science Symposium, 1996. Conference Record., 1996 IEEE.* Vol. 2. IEEE, pp. 702–706.